Evolutionary determination of experimental parameters for ptychographical imaging

SHENFIELD, Alex and RODENBURG, John

Published version

SHENFIELD, Alex and RODENBURG, John (2011). Evolutionary determination of experimental parameters for ptychographical imaging. Journal of Applied Physics, 109 (12), p. 124510.

Evolutionary Determination of Experimental Parameters for Ptycographical Imaging

Alex Shenfield[1, a)] and John M. Rodenburg[2, b)]

[1)] *School of Engineering, Manchester Metropolitan University, John Dalton Building, Chester Street, Manchester, M1 5GD, UK*

[2)] *Department of Electronic and Electrical Engineering, University of Sheffield, Mappin Street, Sheffield, S1 3JD, UK*

The Ptychographical Iterative Engine (PIE) algorithm is a recently developed novel method of Coherent Diffractive Imaging (CDI) that uses multiple overlapping diffraction patterns to reconstruct an image. This method has successfully produced high quality reconstructions at both optical and X-ray wavelengths but the need for accurate knowledge of the probe positions is currently a limiting factor in the production of high resolution reconstructions at electron wavelengths. This paper examines the shape of the search landscape for producing optimal image reconstructions in the specific case of electron microscopy and then shows how evolutionary search methods can be used to reliably determine experimental parameters in the electron microscopy case (such as the spherical aberration in the probe and the probe positions).

Keywords: Parametric Uncertainty; Diffractive Imaging; Evolutionary Computation

[a)]Electronic mail: a.shenfield@mmu.ac.uk

[b)]Electronic mail: j.m.rodenburg@sheffield.ac.uk

I. INTRODUCTION

There has recently been considerable interest in Coherent Diffractive Imaging (CDI), a method by which the intensity of one or more diffraction patterns scattered from an object are processed in order to produce an image of that object. The main field of application for this technique is in the imaging of structures at the atomic scale using X-rays or electrons since, in these cases, it is both difficult and expensive to manufacture good quality lenses of significant numerical aperture. Currently the best aberration-corrected high-energy (200 - 300keV) electron microscopes can only achieve a resolution of approximately 0.05nm[1] despite using electron wavelengths of around 0.002nm. The problem is that the electron lens is required to re-interfere beams which have travelled over substantial laboratory-scale distances (millimetres or centimetres), thus placing extreme demands on its accuracy and physical stability. In contrast, the advantage of diffractive imaging is that the path differences between interfering wave components scattered to different angles by the object are of the order of the atomic separations themselves. Diffraction is therefore experimentally robust and intensity data can be recorded (albeit at low intensity) up to very large scattering angles: i.e. we can, in principle, generate a diffraction-limited *'diffractive lens'* with a very large numerical aperture and hence much better resolution.

In order to produce an image from a Fraunhofer (or Fresnel) diffraction pattern we need to know both its modulus and phase (in order to back-propagate the wave to the object plane via an inverse Fourier transform) - though in practice it is only actually possible to measure the intensity. However, there are now several well-established methods for recovering the phase of a diffraction pattern from its intensity alone. Most of these methods concentrate on the case where either the size of the object is approximately known or when the illumination incident upon the specimen is of a known extent, and a review of the computational approaches - called iterative phase-retrieval methods - applicable when these or similar conditions are fulfilled can be found in Marchesini[2]. In this paper we are concerned with an approach in which many diffraction patterns are recorded from adjacent (but overlapping) areas of an extended object. This principle of using shifting illumination to unlock the phase problem was first postulated by Hoppe[3–6] and is called ptychography: for a review see Rodenburg[7]. Under these circumstances there are both direct (though mathematically ill-conditioned) deconvolution methods[8,9] and modified iterative phase-retrieval ptychography methods[10–12] for solving the phase problem, the latter being extremely efficient, convergent and noise-insensitive. From a microscopists point of view, ptychography also has the great advantage of being able to image objects of any lateral size.

Initially a major limitation of iterative phase-retrieval ptychography was the requirement to have very detailed knowledge of the modulus and phase structure of the illuminating beam (i.e. the probe), with this having to be calculated from estimates of experimental parameters[13]. This is particularly demanding in the case of electron diffractive imaging, where the use of a condenser lens to focus the illumination into a localised area is a requirement, but where the phase of the illumination cannot be measured directly.

However, since this early work, the great redundancy within the ptychographical data set has been shown to allow for the solution of both the object function and the illumination function, at least provided the illumination is substantially localised (so that the Nyquist sampling condition of the diffracted intensity is still satisfied). If the probe positions are known accurately then two techniques have been proposed. One involves projecting alternatively onto two sets (the known diffraction pattern moduli and a set that ensures that the associated exit waves are consistent with a constant object and probe)[12,14]; another is a variation[15] on the original serial weighted update PIE algorithm[16]: these have been compared by Schropp et al.[17]. A more general approach uses a non-linear optimisation iterative search technique[11,18,19], which can in principle cope with any form of measurement error, including errors in the probe positions, assuming the initial experimental conditions lie within a reasonable error envelope. We have found that in the case of electron microscopy achieving high accuracy in the relative probe positions (<0.1nm) is extremely difficult because of specimen drift (movement induced by thermal gradients in the microscope column and stage) and the presence of hysteresis in the beam shift coils[20]. This result is unexpected, since in high-resolution annular dark field imaging (ADF) it is routinely possible to raster scan the beam with sub-atomic precision; however, in testing five electron microscopes from three leading manufacturers, we have found that when the beam shift is large (1-10nm) - as required for ptychography - the accuracy of the probe positioning is poor and irreproducible.

In this paper we first examine the shape of the search landscapes for finding an optimal image reconstruction (a minimum in the error metric) in the specific case of electron microscopy, and discover that it certainly contains many local minima even in the absence of noise. In this context, the illumination function is created by a slightly defocused beam cross-over and can be parametized by a limited number of variables: the angular size (or numerical aperture) of the lens aperture, the spherical aberration constant of the lens and the degree of defocus. We also examine the search space for probe position inaccuracy which, as described above, currently seems to be the biggest single source of error for electron ptychography. We go on to show how an evolutionary approach to this optimisation problem in this context can reliably determine the global minimum in the error metric. The specimen object and probe wave function used in these simulation experiments are shown in Figure 1, and it can be seen that both the modulus and phase of the specimen object contain highly structured information.

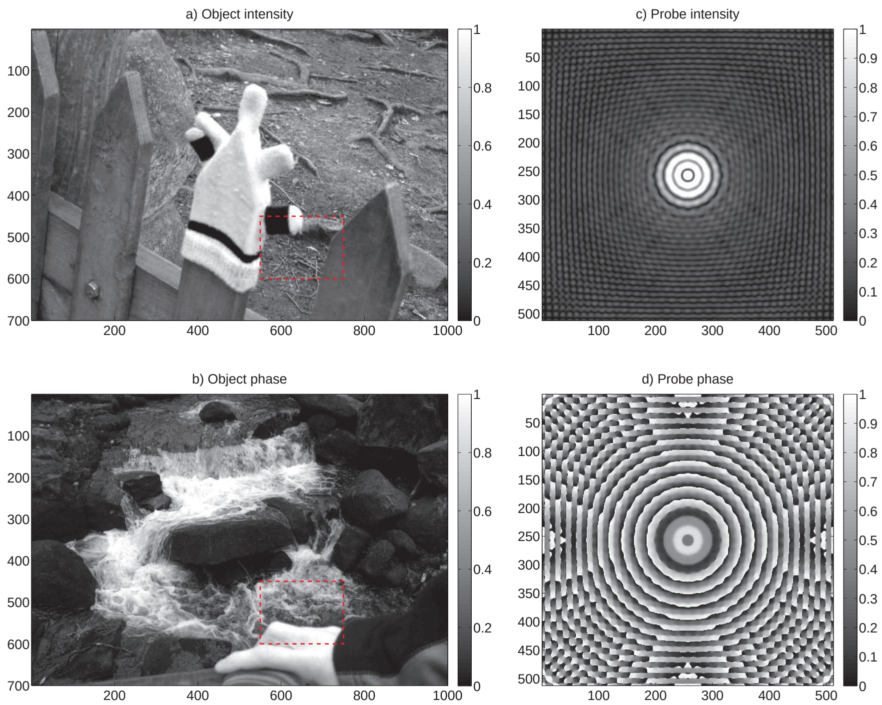

FIG. 1: Images of the object and probe used throughout this paper: (a) shows the intensity of the object, (b) shows the phase of the object, (c) shows the intensity of the probe used to generate the diffraction data, and (d) shows the phase of the probe. In both (a) and (b) a region of 150 by 200 pixels is highlighted. This region contains highly structured data and will be used when comparing the results of the reconstructions produced by the evolutionary approach outlined in this paper.

II. ITERATIVE PHASE-RETRIEVAL PTYCHOGRAPHY

The fundamental concepts of iterative phase-retrieval were first proposed and demonstrated computationally by Gercheberg and Saxton[21]. Essentially these algorithms use both measured data and *a priori* knowledge about the experimental set up to iteratively refine guesses about the complex wavefield until the guessed wavefield matches the recorded data and the *a priori* knowledge about the experiment. For iterative phase-retrieval ptychography the essential constraint is that, as the illumination (i.e. the probe) is moved across the object, all the measured diffraction patterns (Fraunhofer or Fresnel) must be consistent with a single object transmission function: the key is the redundancy in the data resulting from the overlap of adjacent illumination areas on the object. The particular algorithm we employ is called a ptychographical iterative engine (PIE)[10] and uses a weighted update function[16] to account for soft-edged probes. An extended version of this algorithm, ePIE[15], can solve for the illumination function as well as the object function, but only provided that the probe positions are known very accurately: so far inapplicable in electron microscopy given inherent experimental errors. In all that follows we therefore use the PIE algorithm.

III. EFFECTS OF PARAMETRIC UNCERTAINTY IN ITERATIVE PHASE RETRIEVAL PTYCHOGRAPHY

A. Uncertainty in Characterising the Illumination Function

First we consider uncertainty arising from limited knowledge of the probe function. Assuming the absence of astigmatism, which is relatively easy to remove experimentally, we need accurate values for the defocus, spherical aberration and aperture size of the probe forming lens in the STEM (scanning transmission electron microscope) configuration. Whilst aperture size can usually be calibrated within a few percent using the diffraction pattern from a known crystal, it is more difficult to get precise estimates for defocus and spherical aberration. The optical model we use to generate the probes used in this paper can be found in Kirkland[22].

Faulkner and Rodenburg[23] have shown that inaccuracies in any of these characteristic parameters can have a seriously detrimental effect on the quality of the reconstruction produced by the algorithm. However, whilst they showed that the scaled diffraction space error produced by the algorithm improves monotonically as the value of a given parameter becomes more accurate, we have now found that this is only true across a limited range around the true value. Figure 2 shows that the search landscape is actually highly multi-modal when considering a large range of uncertainty.

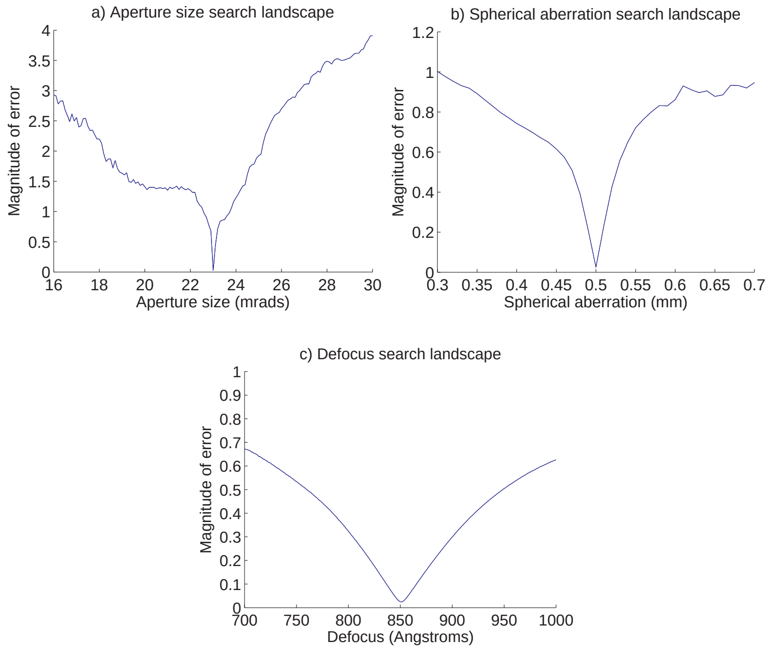

FIG. 2: Search landscapes for the characteristic probe forming parameters over extended ranges: (a) shows the search landscape for the aperture value over an extended but experimentally possible range of errors, (b) shows the search landscape for the value of spherical aberration, and (c) shows the search landscape for the value of defocus. As can be seen from the figure, (a) is highly multimodal whilst (b) and (c) are better behaved.

Further simulations have also shown that the assumption that the error decreases monotonically is also untrue if uncertainty exists in multiple probe forming parameters. This cumulative experimental uncertainty was investigated using a simulated 3 by 3 grid of diffraction patterns (generated by stepping a model of a STEM probe across an image and recording the diffraction data) and looking at the cumulative effects of both small and large errors on the search landscape after 200 iterations of the PIE algorithm. Known errors were applied simultaneously to two of the characteristic parameters under consideration whilst the third was varied across a range of possible values (from approximately -15% to +15% of its true value). This allowed us to study the effect of varying the aperture size (for example) on the search landscape whilst the spherical aberration and defocus simultaneously exhibited both small errors (plus and minus 5% of their true values) and large errors (plus and minus 10% of their true values). The results of this experimental model are shown in Figure 3 (with the vertical lines on each plot representing the true value of each parameter). These results show that only the aperture size is insensitive to cumulative uncertainty in the other characteristic parameters. Both spherical aberration and defocus can be seen to be highly sensitive to this cumulative uncertainty, with the true parameter value not recoverable from either of these figures.

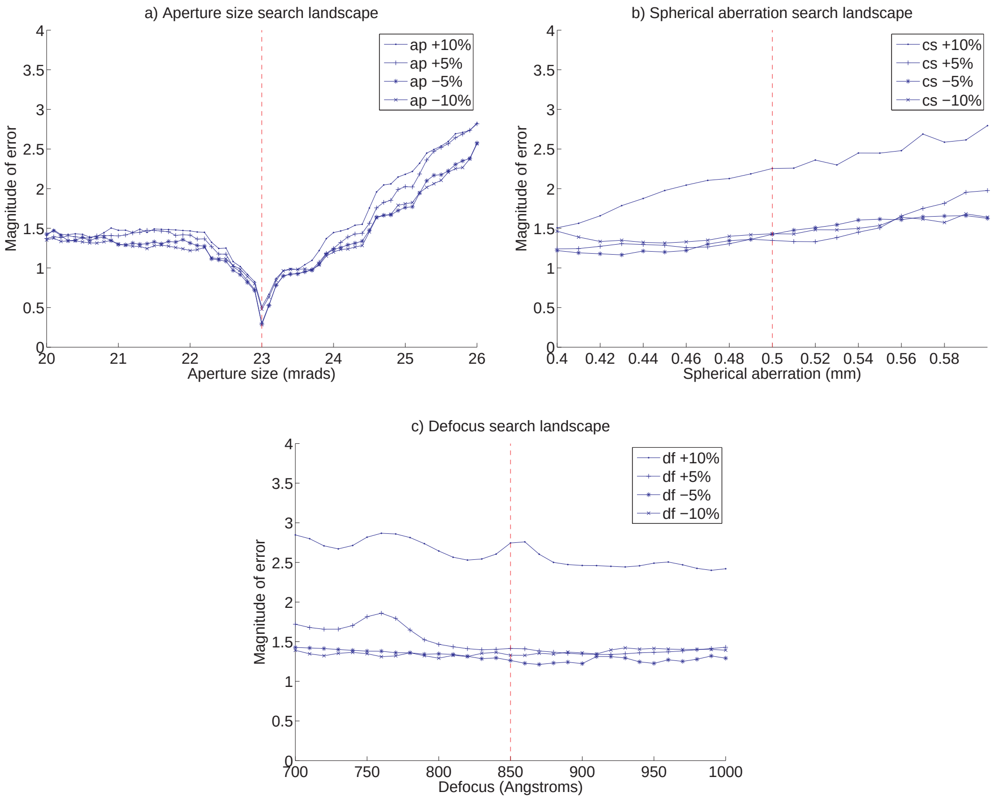

FIG. 3: Error landscapes for the characteristic parameters over large ranges with cumulative experimental uncertainty: (a) shows the effects of this cumulative uncertainty on the error when the aperture size is varied across a range of possible values, (b) shows the effects of this uncertainty on the error when the spherical aberration is varied across a range of possible values, and (c) shows the effect of this cumulative uncertainty on the error when the defocus is varied across a range of possible values. The vertical lines on each plot show the true value of the parameter.

B. Uncertainty in the Positions of the Illumination Functions

Faulkner and Rodenburg[23] have shown that the PIE algorithm is highly sensitive to parametric uncertainty in the probe positions, although in varying only one probe position at a time they concluded that the scaled diffraction space error produced by the PIE algorithm decreased monotonically around the true value of the illumination function position and is thus straightforward to correct using conventional optimisation methods such as gradient descent. However, further simulations presented here show that this is only the case when uncertainty exists in a single position - a situation that has proved to be highly unlikely experimentally (especially when collecting diffraction data from many illumination function positions). When uncertainty exists in multiple illumination function positions, the cumulative effects lead to false minima such as those shown in Figure 4.

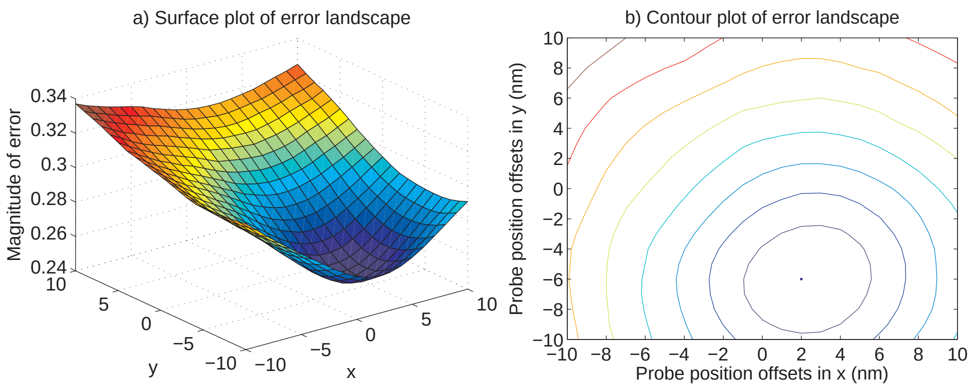

FIG. 4: Effect of multiple probe positions offsets on the scaled diffraction space error: (a) shows the three dimensional surface plot of this error landscape whilst (b) shows the contour plot of this error landscape. The minimum error in this experiment is found at [2, -6].

In this experiment the illumination function used was of the form of a defocussed (STEM) probe (see Figure 1 for the modulus and phase of the probe wave function), as employed in practical electron ptychographical experiments. A 3 by 3 grid of diffraction patterns was generated by stepping the simulated STEM probe across an object and at each point calculating the diffraction pattern by recording the intensity of the Fourier transform of the exit wave emanating from the object (i.e. the product of the probe function at that position and the complex specimen transmission function). Random offsets in the range plus or minus 5 pixels were then applied in both **x** and **y** directions to the recorded positions of every probe except the central one so as to simulate inaccurately known probe positions. The position of this central probe was then varied by increments of one pixel to cover the range minus 10 pixels to plus 10 pixels from its true value in both **x** and **y** directions, and the value of the scaled diffraction space error was recorded. As can be seen from Figure 4, the minimum error is found when the offset of the central probe from its true position is at [2, -6] pixels. This shows that the cumulative effect of uncertainty in multiple probe positions can lead to complex behaviour.

IV. EVOLUTIONARY REDUCTION OF PARAMETRIC UNCERTAINTY

Having explored the problem space in Section III and established its complexity, we will now introduce an evolutionary approach to resolving this parametric uncertainty that is robust to the complex and interdependent nature of the error landscape. This evolutionary approach is then used to resolve the two main sources of error in the reconstruction process: the accuracy of the probe forming characteristic parameters (such as the spherical aberration and defocus) and the knowledge of the probe position information used to generate the set of diffraction data.

A. Introducing an Evolutionary Approach to Resolving Parametric Uncertainty

Evolutionary Algorithms (EAs) are a novel optimisation technique utilising concepts from natural selection[24] to provide a highly robust search method capable of finding global optima in even complex and multi-modal search landscapes. They are both an iterative and population based search method that mimics nature to both explore the solution space of a problem and exploit promising solutions discovered in previous generations. Exploration of the search landscape is performed using recombination and mutation operators that introduce an element of randomness into the search and help ensure the robustness of the algorithm by preventing premature convergence to local optima. Exploitation of promising solutions from the previous generation is performed using a selection operator that ensures preference is given to those solutions that have high fitness values when creating the next generation. In this way we can ensure that the most promising solutions are more likely to make up a significant proportion of the next generation, thus promoting convergence.

The evolutionary approach to resolving parametric uncertainty in iterative phase retrieval methods introduced in this paper is based around evolutionary algorithms with the capability to use both integer and real valued representations for the decision variables. Fogel and Ghoziel[25] have shown that there is no intrinsic advantage in using one representation over another and so modern EA practice emphasises choosing a representation that fits the problem under consideration[26]. In this case that means using an integer representation for the evolutionary refinement of probe positions (see Section IV C) and a real-valued representation for the optimisation of the characteristic parameters used to model the probe (see Section IV B).

Selection in our algorithm was performed using Stochastic Universal Selection[27] since it guarantees sampling with zero bias and is therefore considered superior to other selection schemes for the majority of applications[28]. Recombination and mutation were performed using Simulated Binary Crossover and Polynomial Mutation[29] respectively since these variation operators have been shown to perform well in both the optimisation of real-valued variables and the optimisation of integer variables[30].

B. Evolutionary Discovery of Probe Characteristics

Figure 5 shows a reconstruction using an incorrect probe model generated using characteristic parameters with 2.5% errors in them (a value that is not unlikely under experimental conditions). This Figure shows that, even with these small amounts of uncertainty, the resulting reconstruction is of extremely poor quality with many probe artefacts.

The evolutionary approach to resolving parametric uncertainty introduced in this paper has been used to refine information about the characteristic parameters used to model the illumination function. In this case, upper and lower bounds are set for each parameter based on the estimated precision of the experimentally obtained values. The evolutionary algorithm is then used to obtain accurate values for these probe forming parameters.

Figure 6 shows the progress of our evolutionary approach to resolving uncertainty in the characteristic probe forming parameters. Again we use a 3 by 3 grid of diffraction patterns. We have then simulated large potential margins of error in each of the parameters

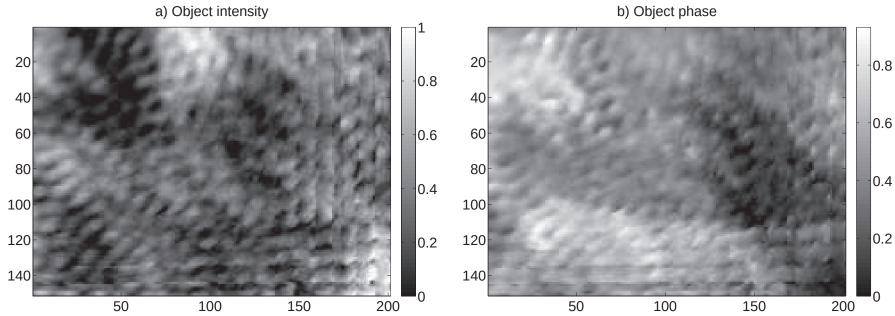

FIG. 5: A reconstruction using a probe model formed with typical experimental errors in the characteristic parameters (this image shows the dotted area from Figure 1). This reconstruction has 2.5% errors in the aperture size, the spherical aberration, and the defocus values used to model the probe. Note that the contrast in this image has been rescaled so that 1% of the data is saturated at low and high intensities to make it suitable for publication.

used in our model by using maximum and minimum bounds for each parameter of plus and minus 25% respectively. Although it is unlikely that the estimated precision of the values would be so poor in a real world experimental situation, using such large ranges provides a good demonstration of the power of our evolutionary approach. Accurate values for these characteristic probe forming parameters are then found by running the evolutionary algorithm for 100 generations.

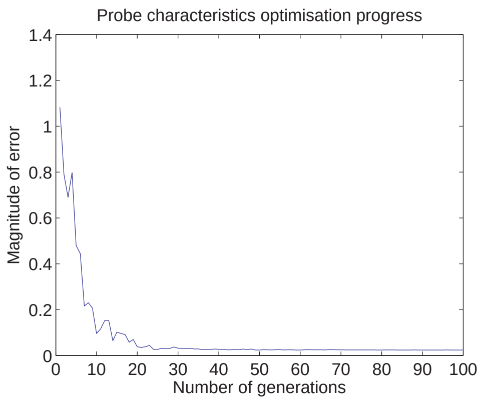

FIG. 6: The progress of our evolutionary approach to reducing uncertainty in the characteristic probe forming parameters. Full convergence can be seen after around 70 generations.

Figure 7 compares the reconstruction produced using the parameters found by our evolutionary approach after 100 generations to the true intensity and phase of the object. This Figure just shows the areas highlighted on Figure 1 where the presence on highly structured information can cause problems for the reconstruction process if there are any inaccuracies in the input information. As can be seen from comparing the reconstructed intensity and phase to the true intensity and phase, the evolutionary algorithm has recovered extremely good values for the probe forming parameters (within 0.2% of the true values). There are no probe artefacts like we can see in Figure 5.

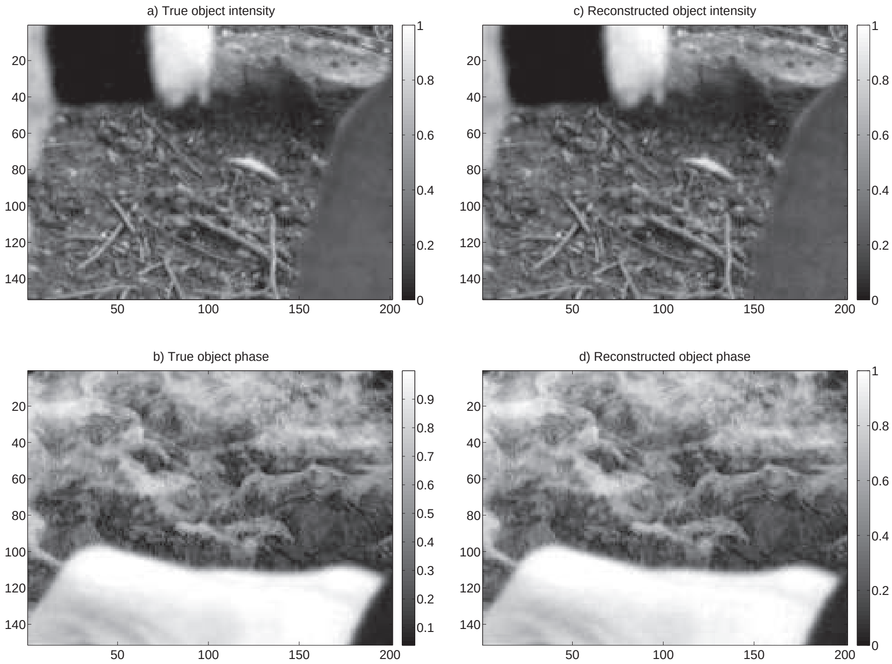

FIG. 7: A comparison of the true object and the reconstruction produced by using the characteristic probe forming parameters found by the evolutionary approach: (a) and (b) show close ups of the true intensity and phase of the object respectively, whilst (c) and (d) show the intensity and phase of the reconstructed object. Note that this figure shows the dotted area from Figure 1.

C. Evolutionary Refinement of Probe Position Information

In this Section our evolutionary approach to the resolution of parametric uncertainty will be used to refine the probe position information and thus improve the results of the reconstruction; this is important as, in the case of scanning transmission electron microscopy especially, it can be difficult to obtain highly accurate information about the position of the specimen stage. A set of simulated diffraction patterns is generated using a 3 by 3 grid of STEM probes with known intensity and phase. Uncertainty is then introduced into the probe position information by applying random offsets of between plus and minus 5 pixels to both the **x** and **y** directions of each probe position. Figure 8 shows the resulting reconstruction from using this incorrect data. Both the intensity and phase reconstructions can be seen to lack clarity as a result of this uncertainty.

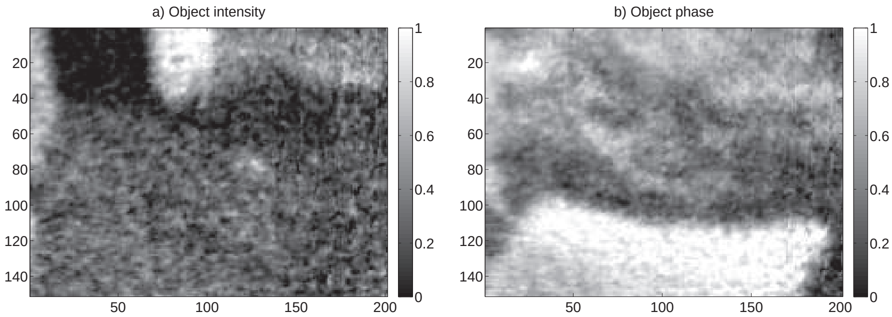

FIG. 8: Reconstruction using uncertain probe positions (this image shows the dotted area from Figure 1). This reconstruction has randomly applied offsets in the range of plus and minus 5 pixels to every recorded probe position in both **x** and **y**, representing realistic experimental errors. Note that the contrast in this image has been rescaled so that 1% of the data is saturated at low and high intensities to make it suitable for publication.

The inaccurate probe position information used in the reconstruction shown in Figure 8 is then refined using the evolutionary approach outlined in Section IV A to minimise the scaled diffraction space error produced by the PIE algorithm after 200 iterations. As can be seen from Figure 9, the algorithm converges to a minimum after around 70 generations. Figure 10 shows a comparison of the true object and the reconstruction after the refinement of the probe position information. Comparing Figures 8 and 10 shows that the refinement of these probe positions has much improved the clarity and detail of the image in both intensity and phase. By further looking at the exact offsets found by this evolutionary refinement of the probe positions we can see that we have successfully recovered the true relative probe positions.

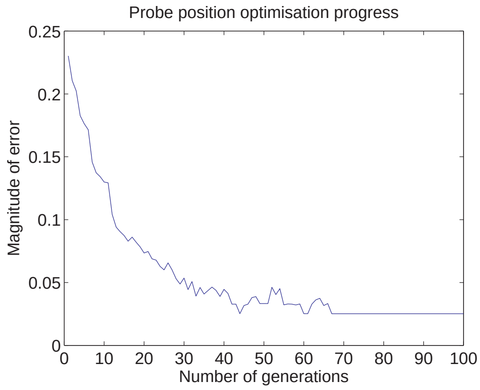

FIG. 9: The progress of our evolutionary approach to reducing uncertainty in the probe positions. Convergence can be seen after around 70 generations.

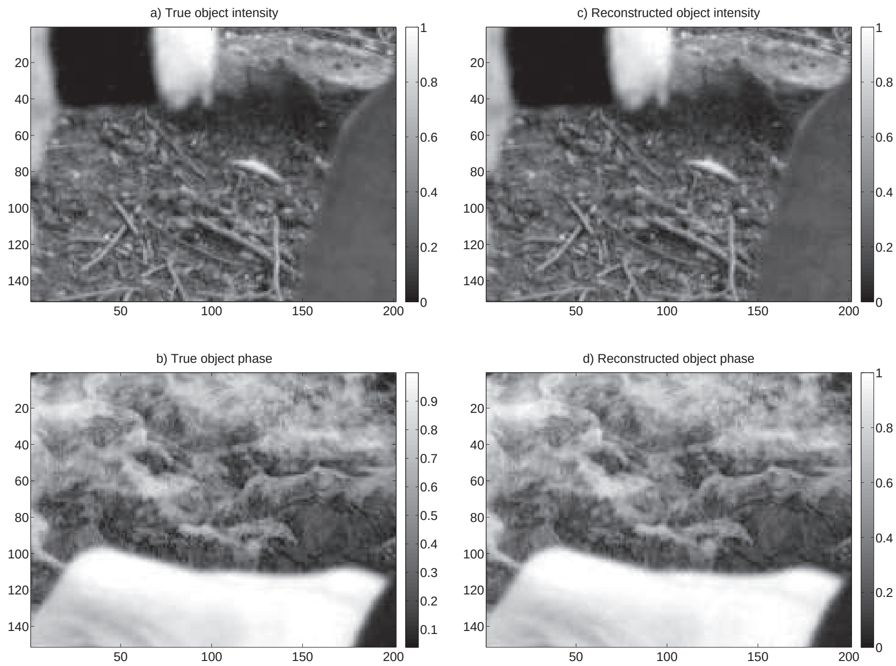

FIG. 10: A comparison of the reconstruction produced by using the probe positions found by the evolutionary approach and the true object: (a) and (b) show a close up of the intensity and phase of the reconstructed object respectively, whilst (c) and (d) show the true intensity and phase of the object. Note that this figure shows the dotted area from Figure 1.

V. CONCLUSIONS

The results presented in this paper have shown that evolutionary optimisation techniques can be effectively used for the resolution of parametric uncertainty in iterative ptychography. Using this approach, we were able to successfully recover and refine information about both the positions of the illumination functions used to generate the diffraction data and the characteristic parameters used to model these illumination functions. This enhanced information has resulted in substantial improvements in the quality of the reconstructions produced by the PIE algorithm, with noticeably higher levels of detail and clarity in the resulting images.

A key factor in the speed of this technique is the estimated precision of the experimental parameters. Although Section IV B has shown that our evolutionary approach can find optimal values for the characteristic parameters over large ranges of uncertainty, knowing the bounds on the parameters with higher precision can very significantly reduce the time taken by the algorithm to obtain good results. For this reason, it is still important to take the utmost care when obtaining the experimental data as this will result in much better performance of the algorithm.

REFERENCES

[1]R. Erni, M. D. Rossell, C. Kisielowski, and U. Dahmen, Physical Review Letters **102** (2009).

[2]S. Marchesini, Review of Scientific Instruments **78**, 011301 (2007).

[3]W. Hoppe, Acta Crystallographica Section A - Crystal Physics, Diffraction, Theoretical and General Crystallography **A25**, 495 (1969).

[4]W. Hoppe and G. Strube, Acta Crystallographica Section A - Crystal Physics, Diffraction, Theoretical and General Crystallography **A25**, 502 (1969).

[5]W. Hoppe, Acta Crystallographica Section A - Crystal Physics, Diffraction, Theoretical and General Crystallography **A25**, 508 (1969).

[6]W. Hoppe, Ultramicroscopy **10**, 187 (1982).

[7]J. M. Rodenburg, Advances in Imaging and Electron Physics **150**, 87 (2008).

[8]J. M. Rodenburg and R. H. T. Bates, Philosophical Transactions of the Royal Society A

- Mathematical, Physical and Engineering Sciences **339**, 521 (1992).

[9]B. C. Mccallum and J. M. Rodenburg, Ultramicroscopy **45**, 371 (1992).

[10]H. M. L. Faulkner and J. M. Rodenburg, Physical Review Letters **93** (2004).

[11]M. Guizar-Sicairos and J. R. Fienup, Optics Express **16**, 7264 (2008).

[12]P. Thibault, M. Dierolf, O. Bunk, A. Menzel, and F. Pfeiffer, Ultramicroscopy **109**, 338 (2009).

[13]J. M. Rodenburg, A. C. Hurst, A. G. Cullis, B. R. Dobson, F. Pfeiffer, O. Bunk, C. David, K. Jefimovs, and I. Johnson, Physical Review Letters **98** (2007).

[14]P. Thibault, M. Dierolf, A. Menzel, O. Bunk, C. David, and F. Pfeiffer, Science **321**, 379 (2008).

[15]A. M. Maiden and J. M. Rodenburg, Ultramicroscopy **109**, 1256 (2009).

[16]J. M. Rodenburg and H. M. L. Faulkner, Applied Physics Letters **85**, 4795 (2004).

[17]A. Schropp, P. Boye, J. M. Feldkamp, R. Hoppe, J. Patommel, D. Samberg, S. Stephan, K. Giewekemeyer, R. N. Wilke, T. Salditt, J. Gulden, A. P. Mancuso, I. A. Vartanyants, E. Weckert, S. Schder, M. Burghammer, and C. G. Schroer, Appled Physics Letters **96** (2010).

[18]G. R. Brady, M. Guizar-Sicairos, and J. R. Fienup, Optics Express **17**, 624 (2009).

[19]M. Guizar-Sicairos and J. R. Fienup, Optics Express **17**, 2670 (2009).

[20]F. Hue, J. M. Rodenburg, A. M. Maiden, F. Sweeney, and P. A. Midgley, Physical Review B **82** (2010).

[21]R. W. Gerchberg and W. O. Saxton, Optik **35**, 237 (1972).

[22]E. J. Kirkland, *Advanced Computing in Electron Microscopy* (Plenum Press, New York, 1998).

[23]H. M. L. Faulkner and J. M. Rodenburg, Ultramicroscopy **103**, 153 (2005).

[24]D. E. Goldberg, *Genetic Algorithms in Search, Optimization and Machine Learning* (Addison-Wesley, Reading, MA., 1989).

[25]D. B. Fogel and A. Ghoziel, IEEE Transactions on Evolutionary Computation **1**, 159 (1997).

[26]Z. Michalewicz and D. B. Fogel, *How to Solve It: Modern Heuristics* (Springer, Berlin, 2000).

[27]J. E. Baker, in *Proceedings of the Second International Conference on Genetic Algorithms*, edited by J. J. Grefenstette (Lawrence Erlbaum Associates, New Jersey, 1987) pp. 14–21.

[28]P. J. B. Hancock, in *Evolutionary Computing - AISB Workshop*, Lecture Notes in Computer Science, Vol. 865, edited by T. C. Fogarty (Springer-Verlag, Berlin, 1994) pp. 80–94.

[29]K. Deb, *Multi-Objective Optimization Using Evolutionary Algorithms* (John Wiley & Sons, New York, 2001).

[30]K. Deb and M. Goyal, Computer Science and Informatics **26**, 30 (1996).

[31]ReferenceNeeded, 0 **0**, 00 (0000).